


Research

Decellularized porcine vena cava grafts are fully repopulated after orthotopic implantation

Richard Palek^{1,2}  · Maria Stefania Massaro²  · Lenka Cervenkova^{2,3}  · Vladimira Moulisova²  · Martina Grajciarova^{2,3}  · Anna Maleckova^{2,3}  · Petr Hosek²  · Jachym Rosendorf^{1,2}  · Robert Polak^{1,2} · Jan Sevcik^{1,2} · Sima Sarcevic^{1,2} · Lucie Kepkova² · Eva Korcakova⁴  · Hynek Mirka⁴  · Zbynek Tonar^{2,3}  · Vaclav Liska^{1,2} 

Received: 19 February 2024 / Accepted: 22 April 2024

Published online: 02 May 2024

© The Author(s) 2024 

Abstract

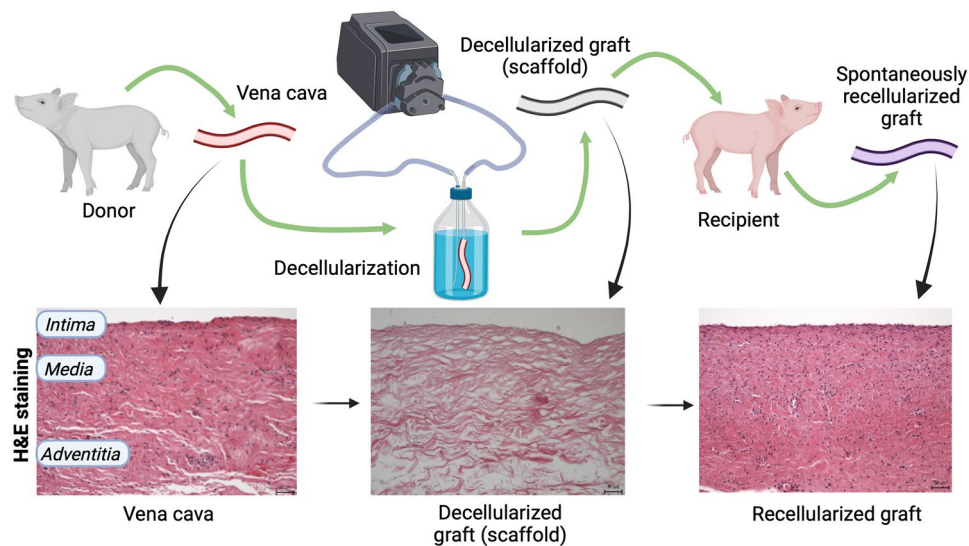
Tissue-engineered organs, based on native extracellular matrix (ECM) scaffolds, could be a game changer in regenerative medicine applications. Decellularization technology provides such scaffolds with organ-typic ECM composition and architecture. Despite limitations such as the requirement of huge cell numbers and finding the optimal route of entry, recellularized scaffolds provide alternative grafts for transplantation. In this study we assessed whether decellularized scaffolds, when implanted, are repopulated from the adjacent tissue. Since the vasculature plays an important role in tissue functionality, our main focus was to evaluate in situ repopulation of decellularized veins in a pig model. For this, porcine inferior vena cava grafts were decellularized and orthotopically implanted in recipient pigs (n = 12). To evaluate possible immune responses to the scaffolds and to assess potential thrombus formation, cellular allogeneic vena cava grafts were transplanted in control pigs (n = 8). Within 28 days after implantation, the decellularized veins were fully recellularized with endothelial cells and smooth muscle cells. Quantitative histological analysis showed a comparable amount of smooth muscle actin in the repopulated decellularized grafts similar to the native IVC. Lymphocyte infiltrates representing signs of graft rejection were not detected in the pigs, as opposed to the control group that received the allogeneic grafts. The decellularized grafts provoked a higher incidence of thrombosis in comparison with allogeneic grafts (33.3 vs. 12.5%). With this study, we show efficient in situ repopulation of decellularized vein grafts. These findings are insightful and promising to further explore the use of decellularized tissue without the need for full pre-transplant recellularization.

Supplementary Information The online version contains supplementary material available at <https://doi.org/10.1007/s42452-024-05910-5>.

✉ Richard Palek, palekr@fnplzen.cz | ¹Department of Surgery, Faculty of Medicine in Pilsen, Charles University, Alej Svobody 80, Plzeň, Czech Republic. ²Biomedical Center, Faculty of Medicine in Pilsen, Charles University, Alej Svobody 76, 323 00 Plzeň, Czech Republic. ³Department of Histology and Embryology, Faculty of Medicine in Pilsen, Charles University, Alej Svobody 76, Plzeň, Czech Republic. ⁴Department of Imaging Methods, Faculty of Medicine in Pilsen, Charles University, Alej Svobody 80, Plzeň, Czech Republic.



Graphical abstract



Article Highlights

1. This study confirms the potential of cell-free decellularized tissue to be fully recellularized in vivo.
2. Decellularized porcine vena cava was repopulated by endothelial and smooth muscle cells after orthotopic implantation.
3. The decellularized vein did not show any signs of immune rejection in contrast to allogeneic cellular graft.

Keywords Decellularized vein · Extracellular matrix scaffold · Vena cava reconstruction · In vivo recellularization · Quantitative histology

Abbreviations

ECM	Extracellular matrix
IVC	Inferior vena cava
SMC	Smooth muscle cells
DMSO	Dimethyl sulfoxide
SDS	Sodium dodecyl sulfate
POD	Postoperative day
AST	Aspartate aminotransferase
ALT	Alanine aminotransferase
ALP	Alkaline phosphatase
GGT	Gamma-glutamyl transferase
CT	Computed tomography
SMA	Smooth muscle actin

1 Introduction

Organ decellularization became an intensively studied topic with a great potential in tissue engineering [1]. An ideal decellularization process enables a gentle removal of all cellular components while preserving an intact extracellular matrix (ECM) containing molecular cues like growth factors and cytokines on its surface. Such ECM or so-called scaffold

has the potential to be repopulated with cells to form an artificial tissue or organ. Using the cells of the potential organ recipient should make the development of immunologically tolerated organs possible [2]. Once this strategy is successful, it could solve the problem of the growing organ shortage in transplantation medicine.

Decellularization has been successfully performed and studied in the case of many organs or tissues like lungs, heart, kidneys, liver, bone, cartilage, vessels, small intestinal submucosa, and many others [1, 3–11]. Some of these organs were also partially recellularized *in vitro* and implanted in animals [6, 7, 12]. However, achieving proper function of such organs and their lifespan after implantation is still a big challenge. The ideal decellularization method, the source of the cells, their sufficient amount, and their optimal delivery into the scaffold are some of the questions that need to be answered before getting closer to the preparation of functioning artificial organs [13, 14].

The creation of a functional vascular system is another critical step for further progress in artificial organ engineering based on native ECM. Therefore it is essential to understand the possibilities of vessel decellularization and recellularization in detail [12, 15]. Moreover, decellularized vessels themselves are a potential alternative to the grafts currently used in cardiovascular surgery [16]. As biological tissues, they should pose a lower risk of infection complications compared to synthetic prostheses [17–19] and their immunogenicity should be minimal compared to allografts [20, 21]. Decellularized matrix can be also used for bioink formulations for construction of vessel grafts through further processing (e.g. bioprinting or electrospinning) where other functionalization such as formation of an antithrombotic layer is possible [22, 23].

The ECM obtained by optimal decellularization preserves bio-inductive properties similar to native tissues. These are the capability of chemotaxis, cell attachment, proliferation, and activation [13, 24, 25]. These unique biomaterial properties together with the structural similarity to the target tissue enable, to a certain level, spontaneous *in vivo* recellularization, which has been observed also in the case of vascular structures [26–28]. A better understanding of spontaneous repopulation of ECM could be beneficial even in whole organ engineering. It could show which type of cells tends to recellularize particular areas of the ECM.

A number of experiments were already performed with decellularized arteries or veins implanted in the arterial system [28–32]. Decellularized arteries implanted in the arterial system showed successful endothelization in the majority of the cases and some of the grafts were even recellularized with smooth muscle cells (SMC) [28–30]. However, microcalcifications in the arterial wall or some degree of intimal hyperplasia were also noted [29, 33, 34]. In the case of decellularized veins implanted in the arterial system, only incomplete endothelization was achieved, which could be caused by different architecture and a biomechanical mismatch between the venous and arterial walls [32, 35].

Very limited experience has been gained with decellularized veins implanted in the venous system [36–38]. In this setting, the pressure load on the venous wall by pulsatile arterial blood flow is eliminated, which could facilitate spontaneous recellularization. The lack of such data is probably due to the lesser imperative for finding alternative grafts for venous replacement as vein reconstruction is less often needed in clinical medicine. However, for the purpose of artificial organ engineering, these findings are essential and could enable further progress. Therefore, we designed an animal model to understand the behaviour of decellularized veins *in vivo* under physiologic conditions. The aim was to investigate the capability of large-diameter decellularized venous grafts to be spontaneously recellularized and to reveal the potential changes in their micro-architecture after implantation. To precisely evaluate these parameters together with the immunogenicity and thrombogenicity, the decellularized vena cava grafts were compared with standard cryopreserved allografts in a porcine model.

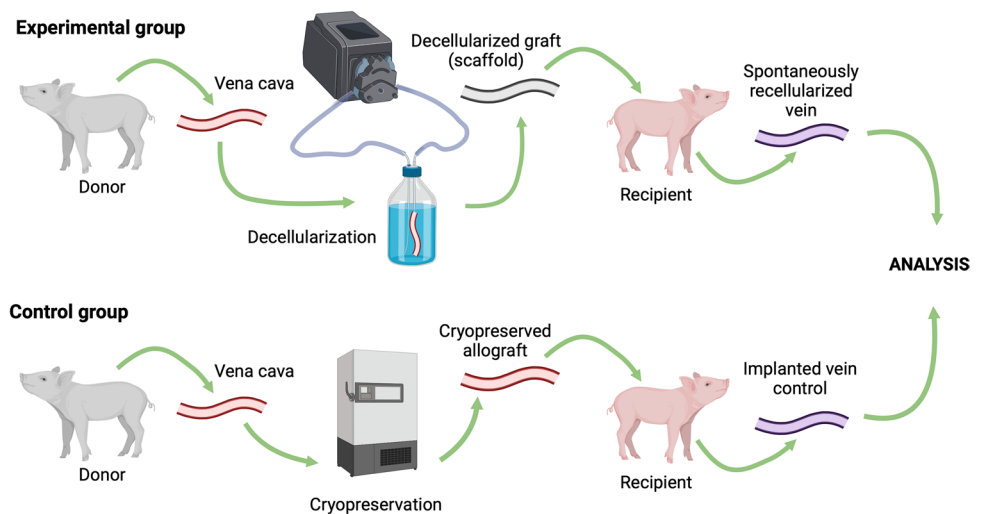
2 Methods

2.1 Experimental animals

In total 40 pigs were used for the experiment (healthy both male and female Prestice Black-Pied pigs, 26.5 to 38.5 kg). Inferior vena cava (IVC) grafts were harvested from 20 donor pigs. Twelve of these grafts were decellularized and then orthotopically implanted in the IVC of the recipient animals from the experimental group ($n = 12$), whereas 8 grafts were cryopreserved and then implanted in the recipient animals from the control group ($n = 8$). The concept of the experiment is depicted in Fig. 1. The recipient animals were then observed for 28 days after implantation. All animals were acclimatized before the experiment, they were fed twice a day and had unlimited access to water. All the surgical procedures were performed under general anesthesia using sterile material.

The protocol of *in vivo* experiment was approved and controlled by the Ministry of Education, Youth and Sports of the Czech Republic (project code: MSMT-18870/2020–3). All the procedures involving animals were performed in compliance

Fig. 1 Scheme of the experimental design. The preparation of the decellularized vena cava, its implantation and sampling (top part) as well as parallel procedures for control cryopreserved vena cava implants (bottom part). Created with BioRender.com



with the law of the Czech Republic, which is compatible with the legislation of the European Union (EU Directive 2010/63/EU for animal experiments).

2.2 Graft harvesting

The donor animals ($n = 20$) received premedication by subcutaneous administration of ketamine (10 mg/kg, Narkamon—Spofa, a.s., Prague, Czech Republic), azaperone (5 mg/kg, Stresnil—Jannssen Pharmaceutica NV, Beerse, Belgium), and atropine (1 mg/animal, Atropin Biotika—Hoechst Biotika, Martin, Slovak Republic). After cannulation of a peripheral vein, general anesthesia was induced by intravenous administration of propofol (1% mixture, 5–10 mg/kg/h Propofol, Fresenius Kabi, Halden, Norway), and the animals were mechanically ventilated. Nalbuphine (10 mg/animal, before the operation and repeated every 2 h during anesthesia, Nalbuphin Orpha, Chiesi CZ, Prague, Czech Republic) was used for analgesia and 0.6 mg of amoxicillin-clavulanate (Augmentin, GlaxoSmithKline Slovakia, Bratislava, Slovak Republic) was administered intravenously as prophylaxis. The IVC was dissected from the level of confluence of iliac veins to the lower margin of the liver. All lumbar veins and both renal veins were ligated and 300 international units (IU) of heparin per kg (Heparin, Zentiva, Prague, Czech Republic) were administered intravenously 5 min before IVC explantation. The explanted vein was then flushed with saline to remove all blood. In the case of grafts for decellularization, the IVC was placed in a 10% dimethyl sulfoxide (DMSO) solution and gradually frozen to $-80\text{ }^{\circ}\text{C}$. The allografts for animals from the control group were placed in 1:1 mixture of 6% Voluven (Fresenius Kabi, Halden, Norway) and 10% DMSO mixed in saline and then also gradually frozen to $-80\text{ }^{\circ}\text{C}$.

2.3 Decellularization

Decellularization of the IVC grafts was done by perfusion with 1% Triton X-100 and 1% sodium dodecyl sulfate (SDS) at room temperature. The grafts ($n = 12$) were thawed at $4\text{ }^{\circ}\text{C}$ and then connected to the perfusion tube. The outflow of the vein was secured with a Luer lock adapter and the graft was placed in a 0.5 L glass bottle with inflow and outflow tubes going through the bottle cap. The following runs of perfusion (50 ml/min) enabled decellularization of the graft: 1 run of saline for 10 min; 2 runs of Triton X-100, each for 60 min; 2 runs of SDS, each for 60 min; and 4 runs of saline, each for 15 min. The solutions were changed before each run. A photograph of the system running is in Fig. 3A including the detail of the vein connection (Fig. 3B).

DNA residue content was used to determine the decellularization efficacy. Briefly, both native and decellularized samples of IVC weighing 40–50 mg were lyophilized to obtain the dry weight used as a reference to indicate DNA residues as ng/mg dry weight. By drying, we eliminated the differences given by the water content from each sample. Then, tissues were powdered using a mortar and pestle in liquid nitrogen and homogenized in a QIAshredder column (Qiagen, Dusseldorf, Germany). Then, DNA extraction was performed with RNeasy mini kit following the manufacturer's guidelines (Qiagen, Dusseldorf, Germany) and Qubit reader was used to obtain the final DNA amount.

2.4 Graft implantation

Recipient animals were anesthetized using the same protocol as in the case of donors. For the prophylaxis, 0.6 mg of amoxicillin-clavulanate was administered intravenously before the operation and repeated 2 h later. Firstly, port-a-cath was implanted to optimize blood sampling and postoperative care. PolyFlow polyurethane catheter was implanted in the right external jugular vein and connected to the ProPort Plastic Venous Access System (Deltec, Smiths Medical International, Ltd., UK) which was placed under the skin on the right side of the neck. Then the abdominal cavity was entered by middle laparotomy, the retroperitoneum was opened by incision of the peritoneum on the right side of the IVC, and the infrarenal part of the IVC was dissected in sufficient length. Several lumbar veins were ligated and transected and attention was paid not to injure the lymphatic vessels running close to the IVC. Five minutes after intravenous administration of heparin (100 IU/kg), the infrarenal IVC was clamped and a 1 to 1.5 cm long segment was resected and replaced with a 1.5 to 2 cm long graft. The decellularized graft was used for experimental animals ($n = 12$) and the cryopreserved allograft for control animals ($n = 8$). Both anastomoses were sewn with continuous 5–0 Prolene suture. After declamping the IVC, the retroperitoneum was left open to prevent fluid collection formation along the reconstruction. The abdominal cavity was closed with interrupted 0 nonabsorbable braided sutures, and 2–0 monofilament nonabsorbable suture was used for skin closure.

2.5 Postoperative follow-up

During the early postoperative period, the animals received infusion of crystalloid solutions (Hartman's and 10% glucose) via the port-a-cath but the access to water was not limited. The dose of feed was gradually increased to the standard dose during the first days. All the animals received 40 mg of pantoprazole every day during the whole postoperative period. No anticoagulants or antithrombotic treatment were used after the operation. The animals were checked every morning to evaluate their overall status.

Blood samples were taken before and after the operation, and then on the 1st, 3rd, 7th, 14th, 21st, and 28th POD. Plasmatic levels of the following markers were assessed in each sample: aspartate aminotransferase (AST), alanine aminotransferase (ALT), alkaline phosphatase (ALP), gamma-glutamyl transferase (GGT), bilirubin, albumin, urea, and creatinine.

Computed tomography (CT) with 20 ml of intravenously administered iodinated contrast agent (Iomeron 350, Bracco, Milan, Italy) with rate of 1.8 ml/s was performed before the operation and then on the 1st, 3rd, 7th, 14th, 21st, and 28th POD.

The abdominal cavity of all the animals was explored under general anesthesia on the 28th POD and the segment of the IVC containing the implanted graft was resected.

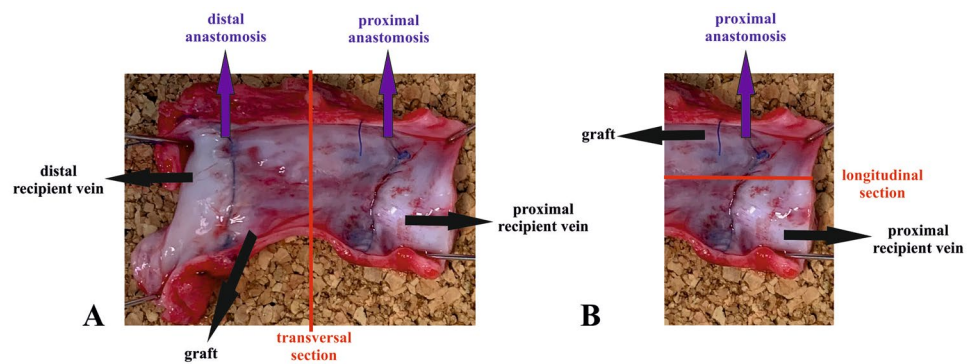
2.6 Samples for histology

Five groups of samples were used for histological analysis: (1) native veins (resected segment of IVC of the recipient, $n = 13$), (2) decellularized veins before implantation (short segment taken from the graft, $n = 12$), (3) cryopreserved veins before implantation (short segment taken from the graft, $n = 8$), (4) decellularized veins after implantation (graft together with both anastomoses and parts of recipient IVC explanted 28 days after implantation, proximal part $n = 7$, distal part $n = 7$), and (5) cryopreserved veins after implantation (graft together with both anastomoses and parts of recipient IVC explanted 28 days after implantation, proximal part $n = 7$, distal part $n = 7$). The number of examined grafts after implantation was lower than the number of grafts before implantation because only the nonoccluded grafts could have been evaluated using the same methodology.

2.7 Histological processing

All venous samples were fixed in 10% neutral-buffered formalin solution. Both decellularized and cryopreserved grafts after implantation were transected in the middle between the proximal and distal anastomosis (Fig. 2A). The samples were then embedded in paraffin blocks following standard histological methods and cut into 5 μm -thick sections (Leica RM2255 microtome, Leica Biosystems GmbH, Nussloch, Germany). Transversal sections were obtained from these samples

Fig. 2 Histological processing of graft samples explanted at the end of the experiment. Decellularized and cryopreserved grafts were transected in the middle between the proximal and distal anastomosis for quantitative histological analysis (A), longitudinal transection was then performed for qualitative histological evaluation (B)



for quantitative histology. Then, the paraffin blocks with veins after implantation were dissolved in order to cut the sample with a longitudinally oriented section plane. The longitudinal sections were then histologically processed for qualitative histological analysis (Fig. 2B). All sections were deparaffinized, rehydrated and stained using the combination of four histological staining methods and four immunohistochemical reactions (Table 1).

Samples of decellularized veins before implantation were not stained with four immunohistochemical reactions (anti-alpha smooth actin, anti-von Willebrand factor, anti-MAC387 and anti-Ki67) due to the absence of cells.

2.8 Microphotographs for stereological analysis

Microphotographs were taken using systematic uniform sampling of the venous wall (Supplementary Fig. 1, Table 1) [39]. The detailed location of these microphotographs is shown in Supplementary Fig. 1. The total number of microphotographs taken and quantified was 2,656.

2.9 Stereological quantification

The design of the quantitative analysis was based on previously published studies on various vessels morphology [40–42]. The area fractions of elastin, collagen and smooth muscle actin were quantified using the stereological point grid and Cavalieri principle [43]. The fractions were estimated as the ratio of the evaluated microscopic structures to the reference area. The settings of the used point grid were in agreement with the standards of stereological methods [44]. The two-dimensional densities of nuclear profiles, vascular profiles and MAC387-positive cells were evaluated using the unbiased counting frame [40, 45]. These densities were estimated as the number of the evaluated structures per reference area. The proliferation index was evaluated as the ratio of Ki67-positive nuclei to all cell nuclei in the reference area. At least 300 nuclei per case were calculated for the proliferation index [46]. Intima-media thickness of veins was measured using four linear probes. Stereological quantifications were performed using the Ellipse software (ViDito, Košice, Slovak Republic). For details see Supplementary Fig. 2.

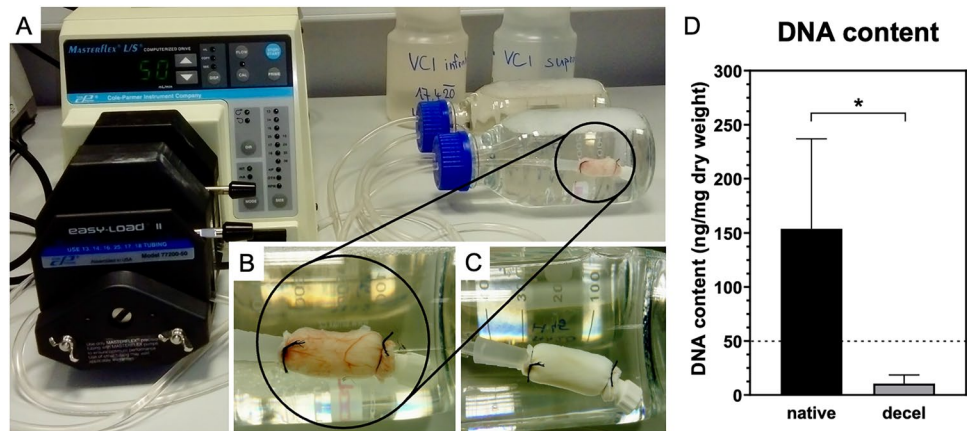
2.10 Statistics

Means and sample standard deviations were used to represent the measured data. Primary analysis of the quantitative histological and biochemistry data was performed with analysis of variance (ANOVA) for repeated measurements, thus respecting the dependency of observations belonging to each animal. In order to maximize statistical power, *post-hoc* analysis was not performed with a complete scheme of all pairwise comparisons, but only biologically relevant comparisons were made using the t-test (either paired or two-sample) with subsequent Bonferroni correction applied to the whole family of test for each variable. In particular, histological variables were compared between all timepoint pairs within each group (3 tests for each group, 6 tests in total) and between the groups at each time point (3 tests) and the Bonferroni-corrected significance level was set to $\alpha_c = 0.05 / 9 = 0.0056$. The exception here was *vasa vasorum*, for which data was not available for the decellularized graft before implantation. The repeated measures ANOVA was thus performed using only the 'native' and '28 days after implantation' timepoints and the post-hoc procedure comprised only 6 tests and $\alpha_c = 0.05 / 6 = 0.0083$. For biochemistry variables, only comparisons between groups (for each time point) were made, resulting in 8 tests and $\alpha_c = 0.05 / 8 = 0.00625$ for each variable. The Bonferroni correction was performed at the

Table 1 Histological staining methods and quantitative parameters

Staining	Quantitative parameter (unit)	Purpose	Evaluated vein	Objective used	Micrographs taken
Verhoeff's method for elastic fibers (Verhoeff 1908)	A_A (elastin, wall) (-)	The area fraction of elastin fibres and membranes	native, decellularized before and after implantation, cryopreserved before and after implantation	40x	4
Picrosirius red (Rich and Whittaker 2005)	A_A (collagen, wall) (-)	The area fraction of type I (yellow-red color) and type III collagen (green color)	native, decellularized before and after implantation, cryopreserved before and after implantation	40x	4
Immunohistochemistry with antibody anti-alpha smooth actin (Clone 1A4, 1:500 dilution, DakoCytomation, Glostrup, Denmark)	A_A (actin, wall) (-)	The area fraction of smooth muscle actin	native, decellularized after implantation, cryopreserved before and after implantation	40x	4
Gill's hematoxylin	Q_A (nuclear profiles, wall) (mm^{-2})	The quantity of nuclear profiles	native, decellularized after implantation, cryopreserved before and after implantation	40x	4
Immunohistochemistry with antibody anti-von Willebrand factor (1:1000 dilution, DakoCytomation, Glostrup, Denmark)	Q_A (vasa vasorum, wall) (mm^{-2})	The quantity of vascular profiles	native, decellularized after implantation, cryopreserved before and after implantation	40x	4
Immunohistochemistry with antibody anti-MAC387 (MA 1-80,446, 1:200 dilution, ThermoFisher Scientific)	Q_A (MAC387-positive cells, wall) (mm^{-2})	The quantity of MAC387-positive cells	native, decellularized after implantation, cryopreserved before and after implantation	40x	4
Immunohistochemistry with antibody anti-Ki67 Clone MIB-1, Ready to use, DakoCytomation, Glostrup, Denmark)	Proliferation index (%)	The ratio of Ki67-positive cells to all cells in the reference area	native, decellularized after implantation, cryopreserved before and after implantation	40x	4
Hematoxylin-eosin (Bancroft 2008)	Intima media thickness (IMT) (μm)	The thickness of tunica intima and media	native, decellularized before and after implantation, cryopreserved before and after implantation	10x	4

Fig. 3 Perfusion decellularization of IVC graft using peristaltic pump (A), detail of IVC graft at the beginning of the decellularization process (B) and at the end of decellularization process (after 310 min of perfusion) (C); DNA content estimated for native veins as well as decellularized scaffolds shows significant reduction in case of decellularized tissue going below the generally accepted limit for decellularized tissue (50 ng/mg dry tissue, dashed line) (D)



level of significance threshold α and if shown, the original p -values are presented. All reported p -values are two-tailed and the general level of statistical significance was set at $\alpha=0.05$. Statistical analysis was performed in Statistica (ver. 12 Cz, TIBCO Software Inc., Palo Alto, CA, USA).

3 Results

3.1 Vein decellularization

Successful decellularization process of the IVC grafts was confirmed by DNA analysis as well as by histology. DNA residues were found to be lower than 50 ng/mg dry tissue for the decellularized vein and significantly lower compared to the native vein (mean 10.63 vs 153.8, $p=0.014$, unpaired t -test) (Fig. 3D). Moreover, any cells or nuclei were not found in the wall of the decellularized grafts based on evaluation of Gill's hematoxylin stained sections (Fig. 6C), making these native scaffolds suitable for the following orthotopic implantation.

3.2 Survival of implanted animals

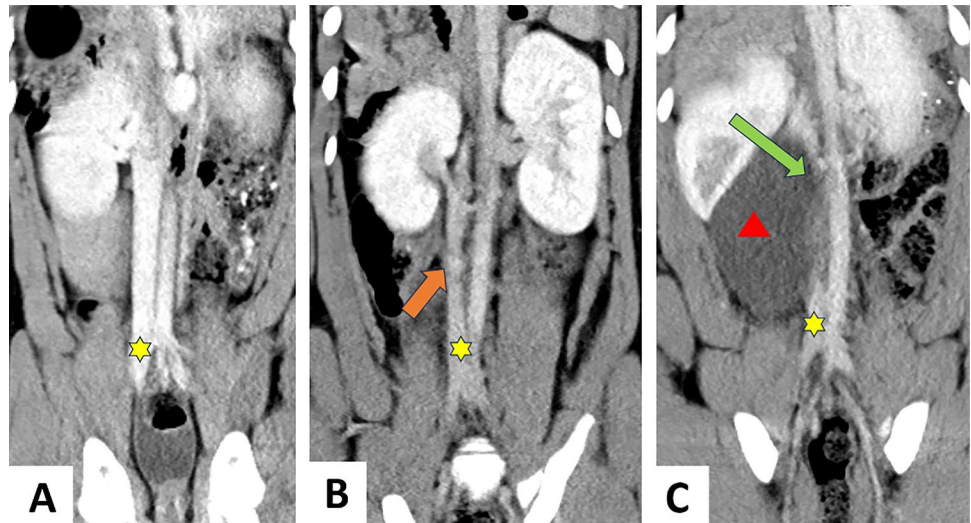
All the animals from the control group ($n=8$) survived the whole period of 28 days after graft implantation. In the case of the experimental group, one out of 12 animals died on the 14th POD. The death occurred a few hours after the CT examination which was done in analgesedation with ketamine and azaperone. Results of the autopsy, CT, and biochemistry did not show any pathology related to the surgical procedure. The IVC graft was patent without any signs of thrombosis.

3.3 Graft thrombosis and CT results

The thrombosis of decellularized IVC graft occurred in 4 out of 12 experimental animals (33.3%). The rate of cryopreserved IVC graft thrombosis was lower, with only 1 animal out of 8 in the control group (12.5%). All observed thromboses were confirmed after explantation of the grafts at the end of the experiment. Additionally, the CT examinations enabled the detection of the time of thrombosis development. The graft thrombosis occurred during the first postoperative week in 3 animals. Exactly, it was observed on CT on the 7th POD in 2 animals and on the 1st POD in 1 animal (all animals with decellularized graft). Later incidence of graft thrombosis was observed on CT on the 14th POD in 2 animals (one with decellularized and one with cryopreserved graft). Two animals with decellularized graft thrombosis had a fluid collection compressing the IVC at the area of graft implantation. Such fluid collection was not apparent on CT scans of the other 3 animals with graft thrombosis. In total, some fluid collection near the implanted graft was present in 5 animals with decellularized grafts and in 3 animals with cryopreserved grafts. Only 2 of these collections did not spontaneously resolve and were accompanied by graft thrombosis in animals with decellularized grafts. Examples of CT results are presented in Fig. 4.

To evaluate the graft diameter and potential stenotic complications preoperative CT was compared with the CT performed on the 28th POD. Only animals without graft thrombosis were included (experimental group with decellularized

Fig. 4 CT scans of the retroperitoneum. An asterisk indicates the IVC. Normal IVC—preoperative CT (A), the decellularized graft implanted in infrarenal vena cava is patent (orange arrow)—CT on 7th POD (B), example of rare occlusion of the decellularized graft (green arrow) compressed by large fluid collection (red triangle)—different animal, CT on 7th POD, graft thrombosis was confirmed at the end of experiment (C)



grafts $n = 7$, control group with cryopreserved grafts $n = 7$). Data from the other time points especially during the first postoperative week were influenced by perioperative changes and fluid collections affecting the IVC diameter. As most of the collections were resolved during the postoperative period, the data from the 28th POD were the most reliable. The diameter of IVC before graft implantation was comparable between the experimental and control groups (mean 11.7 mm and 11.2 mm respectively). Slight narrowing developed due to the graft implantation but the graft diameter 28 days after implantation was comparable in experimental and control animals (mean 8.1 mm and 8.6 mm respectively). The tendency to narrow was not significantly different between experimental and control animals (difference between preoperative IVC diameter and graft diameter on 28th POD—mean 3.6 mm and 2.7 mm respectively). See the data in Supplementary Fig. 3.

3.4 Macroscopic appearance of the grafts

The decellularized grafts appeared to be of slightly softer consistency compared to the cryopreserved grafts. However, the handling and sewing of anastomoses were not really different when comparing decellularized and cryopreserved grafts. Four weeks after implantation, there were adhesions in the retroperitoneum in the area of IVC reconstruction. Just a minimum of adhesions were found between the small intestine and the abdominal wall in a few animals from both groups. In the case of the animals with graft thrombosis, there were several collateral veins in the retroperitoneum which complicated the graft extraction at the end of the experiment. These collaterals were not present at the time of graft implantation. The explanted grafts were cut longitudinally and inspected from the luminal side. The inner side of the implanted grafts was of similar character as the native IVC. There were no macroscopically apparent differences between decellularized and cryopreserved grafts 28 days after implantation (Fig. 5).

3.5 Qualitative histology analysis

The histology analysis also confirmed successful decellularization process in all 12 grafts. The wall of these grafts prior to the implantation did not contain any cells (Fig. 6). In the case of grafts after implantation, the structure of individual layers of the venous wall was relatively preserved in all the samples. Only in the case of cryopreserved grafts 28 days after implantation, the structure was altered by extensive lymphocyte infiltration. On the contrary, decellularized grafts contained only mixed inflammatory infiltrates around the suture material at the area of both anastomoses. All the decellularized as well as cryopreserved grafts were completely endothelized 28 days after implantation (Fig. 7B). Both types of grafts also contained vasa vasorum with endothelized lumen and smooth muscle actin (SMA) positive cells in tunica media. A coherent layer of SMA-positive cells was found only in the wall of the native vein. In the decellularized grafts after implantation, SMA-positive cells were distributed in small groups or separately in the venous wall. In the cryopreserved grafts, SMA-positive cells were located among lymphocyte infiltrates (Fig. 7A). Proliferating cells were located mainly in the cryopreserved grafts in the form of lymphocyte infiltrates. In the decellularized grafts, the proliferating cells were present to a lesser extent only around the suture material or in small groups in the graft wall (Fig. 7C).

Fig. 5 Decellularized and cryopreserved grafts right after implantation (**A, B**), 28 days after implantation—in situ (**C, D**), and 28 days after implantation—view on the luminal side after the longitudinal cut (**E, F**). The arrows show the direction of the blood flow

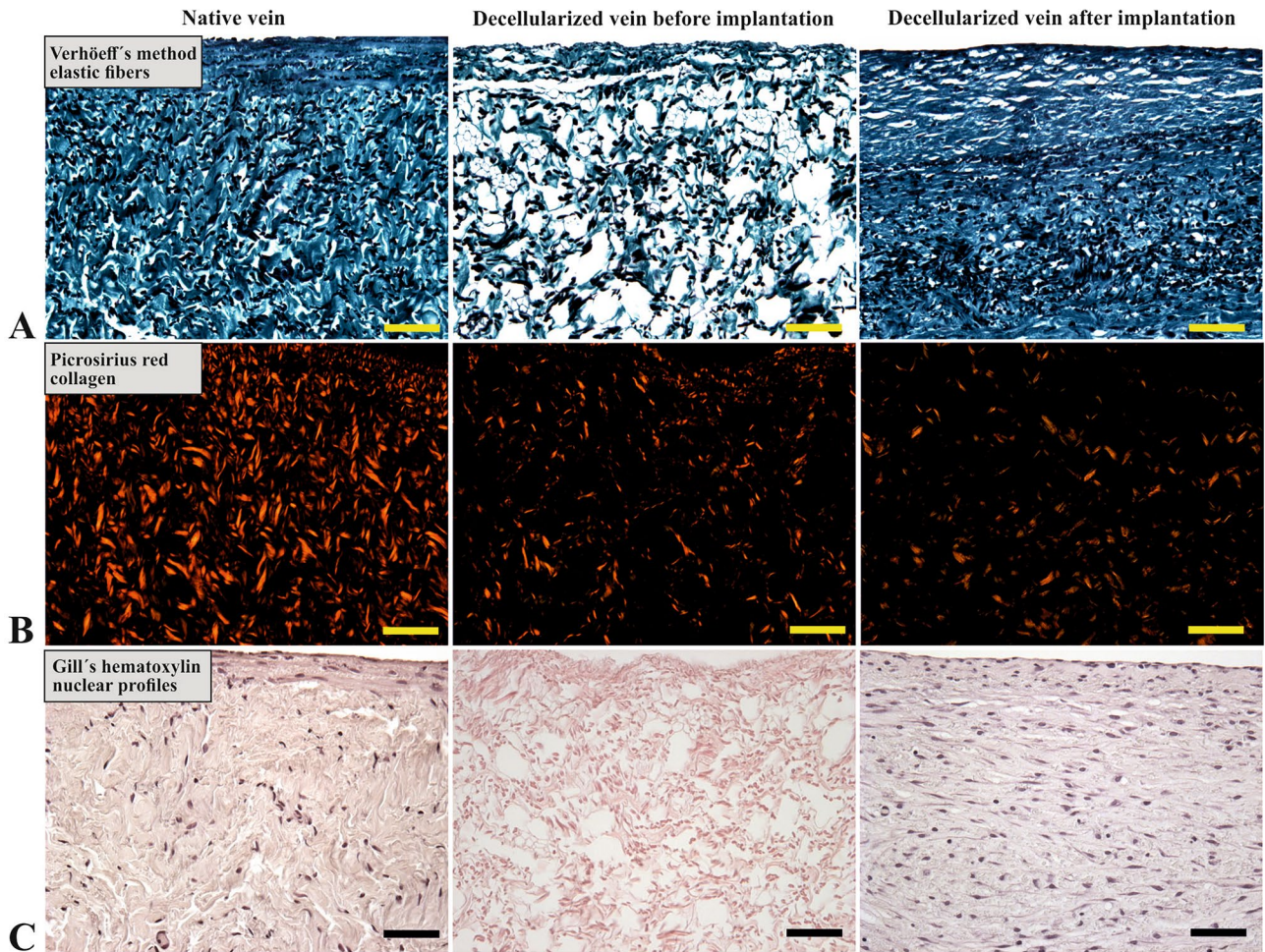
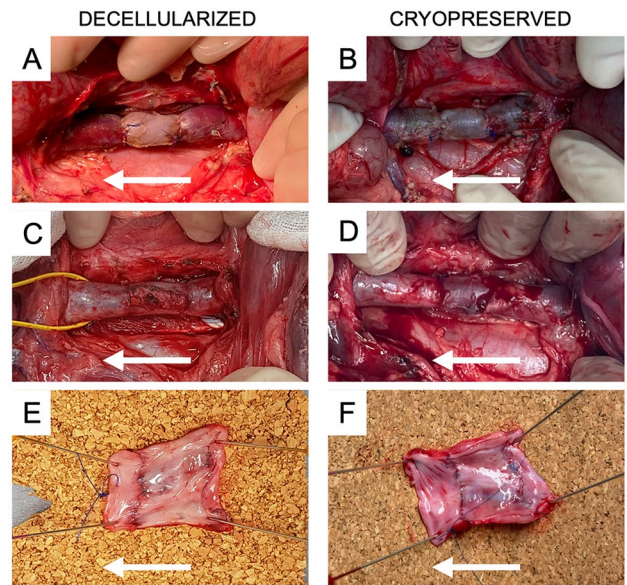


Fig. 6 Histological comparison of the structure of native (left), decellularized (middle) and spontaneously recellularized (28 days after implantation) IVC (right). Verhoeff's green trichrome staining showing elastic fibres in black (**A**) and picrosirius red staining for collagen fibres (**B**) show signal in all, native, decellularized and recellularized samples; Gill's hematoxylin staining detecting purple nuclei depicts nuclei in native and recellularized vein while decellularized sample is nucleus-free (**C**). Scale bars represent 50 μ m in all images

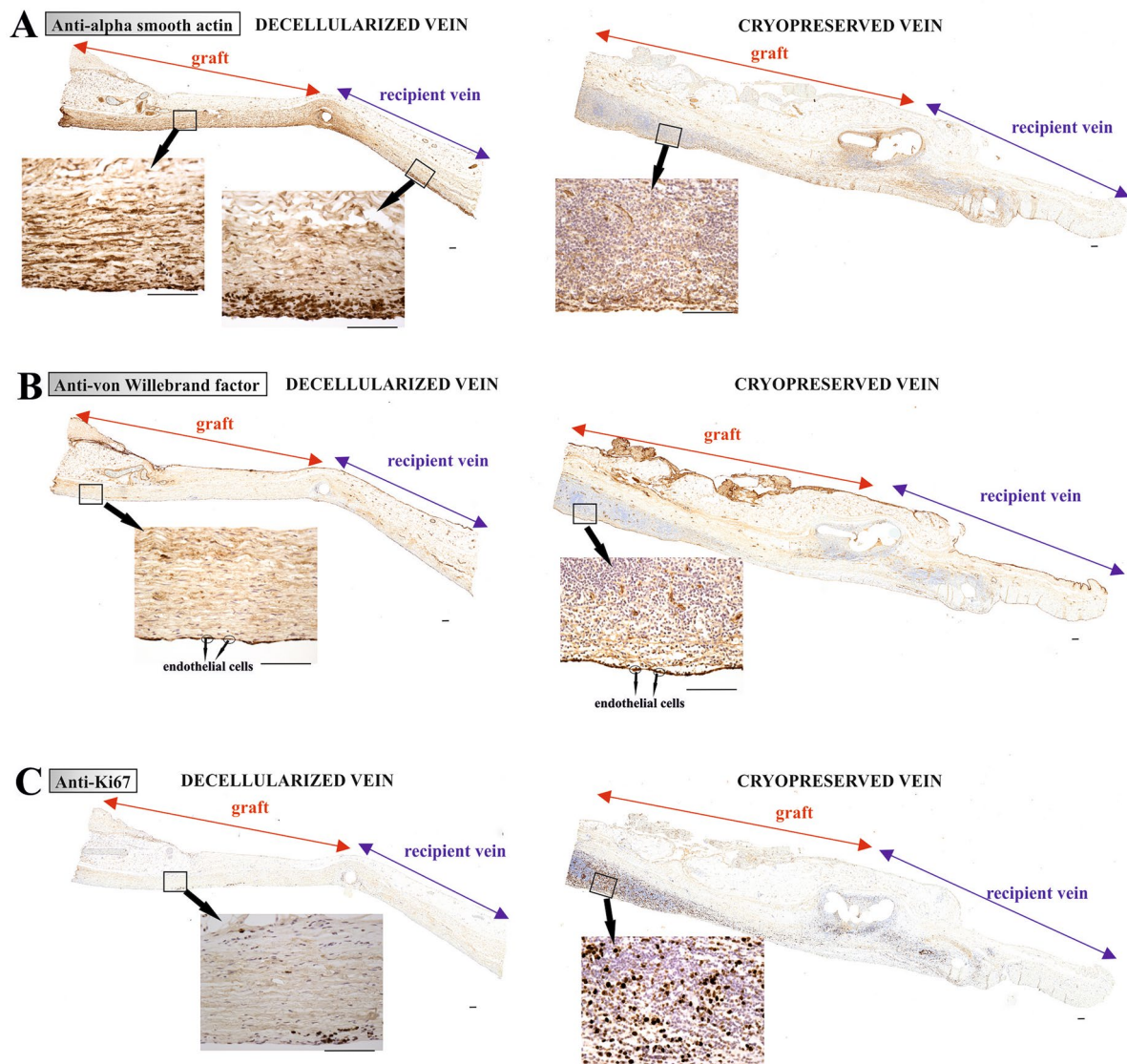


Fig. 7 Microscopic appearance of the decellularized and cryopreserved grafts 28 days after implantation (longitudinal section). In the native veins, smooth muscle cells are arranged in a layer. Decellularized grafts after implantation have smooth muscle cells in groups, and cryopreserved grafts have individual smooth muscle cells scattered among lymphocyte infiltration (A). The newly formed endothelium on the grafts (B). Cryopreserved grafts have more proliferating cells than decellularized grafts (C). Scale bars 100 μ m (A–C)

3.6 Quantitative histology analysis

After qualitative evaluation, quantitative assessment was performed for ECM components elastin and collagen content as well as SMA-positive cells, vessel wall thickness, nuclear profiles, cell proliferation, presence of vasa vasorum and infiltration of macrophages. The area fraction of elastin showed a significant decrease after graft decellularization or cryopreservation and after graft implantation. The proportion of elastin was not significantly different between the groups at any time point (Fig. 8A).

In the case of collagen, there was a significant decrease in the area fraction after the implantation of the decellularized grafts. No significant differences between the groups were observed (Fig. 8B).

The fraction of SMA-positive cells showed a tendency to decrease in cryopreserved grafts during the experiment. The decellularized grafts lost the cells during the decellularization process, but the fraction of SMA-positive cells after implantation reached a similar value as in the native vein (Fig. 8C).

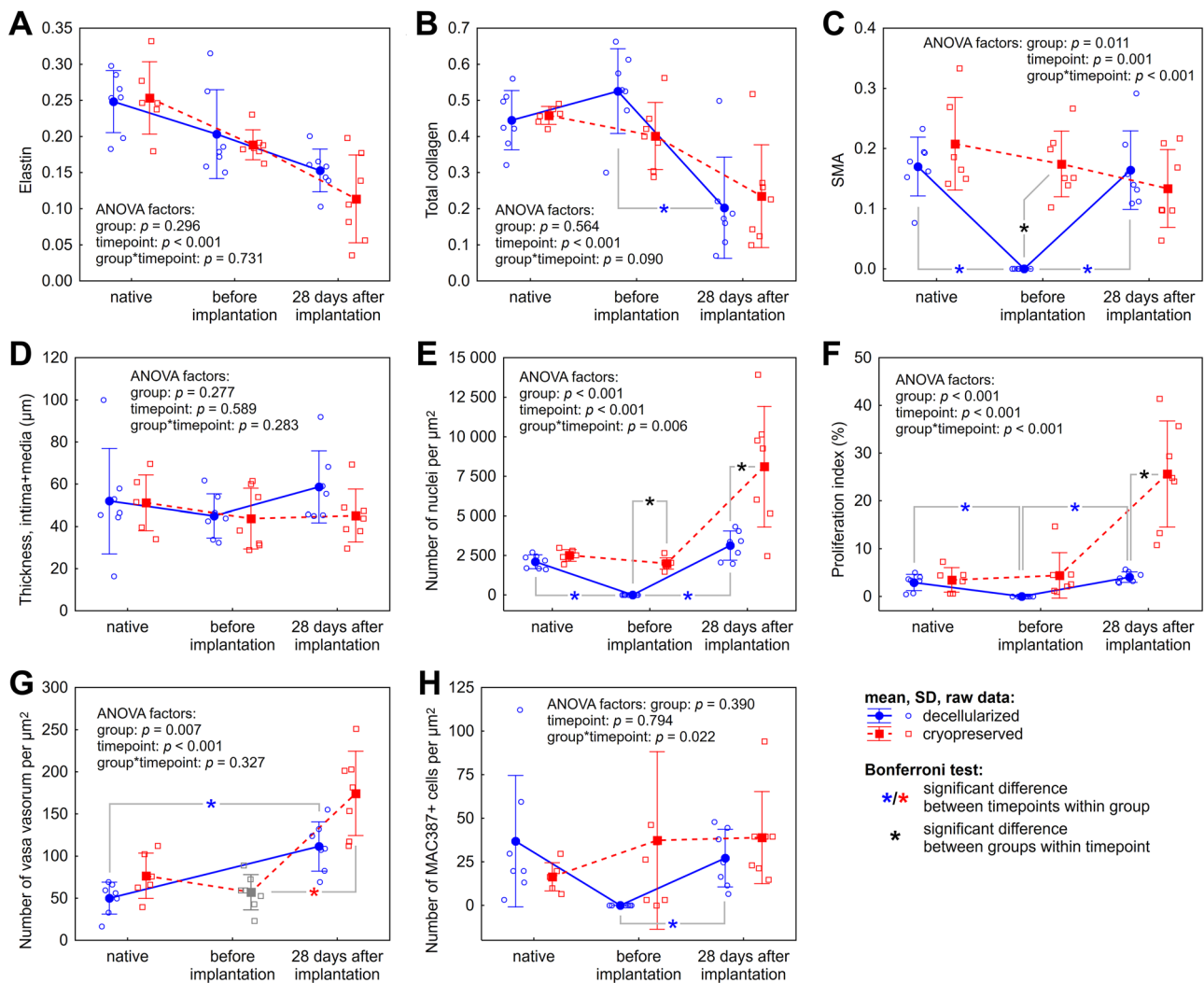


Fig. 8 Visualization of the data from quantitative histology. See comments in the text. Since the data for vasa vasorum (G) was not available for the decellularized graft before implantation, the corresponding time point was excluded from the ANOVA also for the cryopreserved samples (shown in grey). It was, however, included in the manual post-hoc procedure

The thickness of the graft wall did not change significantly during the experiment for any of the groups and was not significantly different between the groups at any time point (Fig. 8D).

In the case of decellularized grafts, the number of nuclei profiles after implantation was comparable with the number found in the native vein. This is proof of cell migration into the graft because the graft after decellularization contained no nuclei. In the case of the cryopreserved grafts, the number of nuclei profiles was significantly higher after implantation, showing a more pronounced lymphocyte infiltration in these grafts (Fig. 8E).

Proliferation index was similar in decellularized grafts after implantation compared to the native vein. Contrarily, the value was multiple times higher in cryopreserved grafts after implantation compared to the native vein (Fig. 8F).

The density of vasa vasorum profiles increased after implantation in both types of grafts compared to the number in the native vein. However, this increase was more pronounced (yet less statistically robust) in cryopreserved grafts, which had a higher density of vasa vasorum after implantation compared to the decellularized grafts (Fig. 8G). Therefore, decellularized grafts after implantation seemed to be less different from the native tissue compared to the cryopreserved grafts.

Besides the expected drop in the decellularized grafts before implantation, the fraction of MAC387-positive cells representing mainly macrophages did not show significant differences with respect to time or graft type (Fig. 8H).

To reveal any potential differences in the graft wall depending on the blood flow, sections from the proximal (caudal), as well as the distal (cranial) part of the graft, were analysed. Decellularized grafts had a greater fraction of total collagen at the proximal part compared to the distal part (mean 0.236 vs 0.169, $p = 0.037$, paired t-test).

Cryopreserved grafts showed a higher amount of MAC 387 positive cells in the proximal part rather than in the distal part (mean 53.3 vs 25.5, $p=0.045$, paired t-test). The other histological parameters did not differ between the proximal and distal area of the graft.

Complete morphologic data are summarized in Supplementary Table 1 and Supplementary Fig. 4.

3.7 Biochemistry

Only one animal from the experimental group which died on the 14th POD was excluded from the biochemistry analysis because of incomplete data. However, the available data of this animal were of similar values compared to surviving animals. There was an elevation of bilirubin on the 1st POD in animals from the control group which was not seen in animals from the experimental group. Similarly, the control animals had elevated level of ALP on the 1st POD and higher levels of ALP compared to experimental animals during the 1st postoperative week (Fig. 9). All the other biochemical parameters (AST, ALT, GGT, albumin, urea, and creatinine) did not show significant differences between the groups and stayed within normal range for the postoperative period [47].

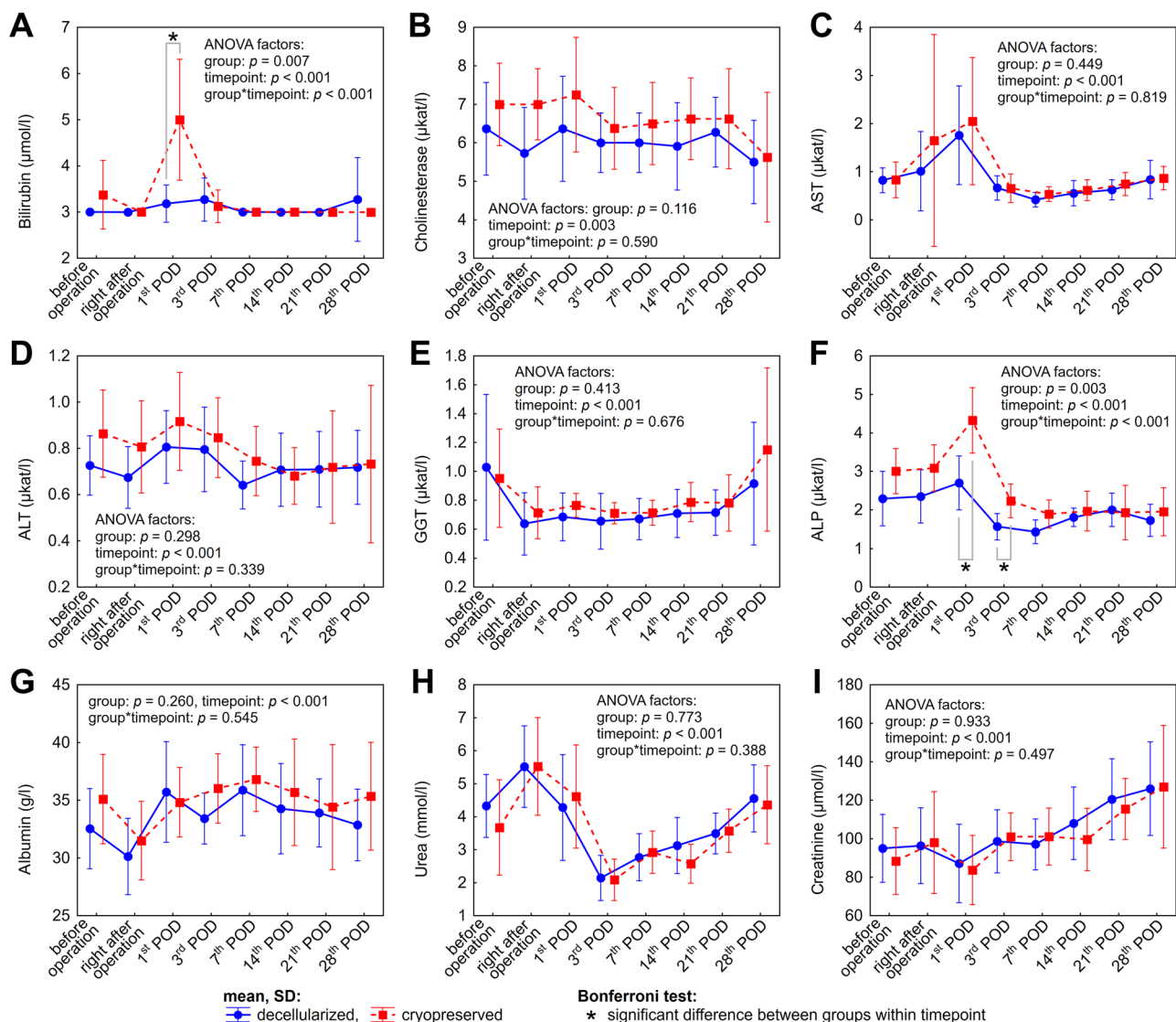


Fig. 9 Results of the biochemistry analysis. Only bilirubin and ALP exhibited differences between groups. Differences between individual time points were not tested in the post-hoc procedure in order to conserve statistical power for the comparison of groups

4 Discussion

There is very limited evidence of the behaviour of decellularized veins implanted *in vivo* under physiologic conditions. Experiments with decellularized vessels are usually designed to evaluate potential alternatives to clinically used grafts for vascular reconstruction. Therefore, the venous grafts are mostly implanted in the arterial system [32, 48, 49]. In such a setting, the venous wall is excessively irritated due to arterial pressure which could alter the spontaneous recellularization. In the case of implantation in the venous system, the wall of the decellularized graft is usually modified prior to the implantation to prevent thrombosis (e.g. heparinization, re-endothelization) [36, 50]. Such modifications could also affect the *in vivo* recellularization process. To study the capacity of spontaneous repopulation of decellularized venous wall, we designed an experiment with orthotopic implantation of decellularized IVC graft without any prior anti-thrombotic modification. To date, mainly graft patency and re-endothelization were evaluated in the published studies [36, 37]. This is the first time to the author's knowledge that quantitative histological analysis of the main extracellular components forming the venous wall is performed in this setting. To evaluate the immunogenicity, we compared the decellularized grafts with cellular cryopreserved allografts.

4.1 Successful decellularization

Normal values of DNA content for porcine vein are higher than 100 ng/mg tissue, reduced to around 5ng/mg tissue in case of decellularization. It is commonly defined in literature that good decellularization leads to DNA content below 50 ng/mg tissue [51]. Our results confirm a good decellularization of the porcine IVC.

4.2 *In vivo* recellularization

The decellularized grafts showed the capability of spontaneous recellularization by endothelial as well as smooth muscle cells 4 weeks after implantation. The amount of SMA was not different from native IVC. The cells repopulated the appropriate locations of the venous wall including endothelization of vasa vasorum.

The *in vivo* repopulation of decellularized vascular structures has been documented in case of arteries implanted in the arterial system. The endothelization is usually successful, but the repopulation of the rest of the vascular wall is not usually studied in such detail [28, 34]. Decellularized ovine carotid arteries showed just limited spontaneous repopulation which was attributed to dense collagen bundles obstructing the cell migration [34].

Results corresponding to our findings concerning successful endothelization and smooth muscle cells repopulation were acquired in experiment with decellularized porcine IVC grafts that were perfused with the recipient's blood prior to implantation. The perfusion took one week, and it was performed with the intent to add the recipient's autologous components to prevent rejection and facilitate *in vivo* recellularization. In the proof of concept study, there were 6 pigs included with short-term survival (3 days to 5 weeks) [37]. The following study evaluates similar grafts explanted after long-term survival of 10 recipient pigs (6 to 13 months) [38]. Compared to these studies we proved the capability of spontaneous recellularization without the need for preconditioning with the recipient's blood, which is technically demanding and increases the costs. The decellularized venous graft itself has sufficient functionality to attract specific cells in the appropriate locations including tunica media and vasa vasorum.

4.3 Histology of ECM

To reveal the potential damage to the vascular wall during decellularization we evaluated the amount of collagen and elastin as the main extracellular proteins. Moreover, changes in the amount of collagen and elastin have been documented in allogeneic venous grafts after implantation [52–54]. Therefore, to properly compare the performance of decellularized grafts with allografts, the quantitative analysis of collagen and elastin content was also performed 28 days after implantation. The amount of collagen and elastin was lower in decellularized as well as cryopreserved grafts after implantation when compared to native IVC but not significantly different between both graft types in any of the time points. The study of Kahle et al. showed an increase of collagen and reduction of elastin/collagen ratio accompanying venous graft disease [52]. They examined cellular allografts implanted in the arterial system. In our study, there was no increase (but rather a decrease) after implantation. Increase of collagen content in the venous wall after implantation in

the arterial system was documented also by other studies [55, 56]. We hypothesize that these changes were prevented by the implantation of the venous grafts in the venous system, thus eliminating irritation by pulsatile arterial pressure. The decrease of elastin proportion, which was observed in the wall of both decellularized and cryopreserved grafts, corresponds to our previous findings. In the experiment with portal vein reconstruction using allografts originating in the portal or caval venous system, we detected a similar decrease in elastin proportion 4 weeks after graft implantation [57].

4.4 Immunogenicity

The cellular cryopreserved allografts showed major lymphocyte infiltration. As the lymphocytes and predominantly T-lymphocytes are known to be responsible for the immune response to implanted vein allografts [58, 59] this finding documents the immunogenicity of cryopreserved grafts in our study. Contrarily the decellularized grafts did not contain any lymphocyte infiltration out of the anastomotic area which proves substantially lower immunogenicity of these grafts. This finding is supported by a significantly higher proliferation index in the wall of cryopreserved grafts 28 days after implantation since the proliferating cells were present mainly in the lymphocyte infiltrates.

The presence of proliferating cells at the anastomotic area of the decellularized grafts corresponds with the finding of Osterberg et al. and is apparently caused by non-absorbable suture material [38].

The MAC387 positive cells represent mainly macrophages which are responsible for non-immune inflammation as crucial regulators of tissue healing [60]. There was no difference in the amount of MAC387-positive cells between animals with cryopreserved or decellularized grafts.

4.5 Intimal hyperplasia

Bai et al. have studied decellularized grafts of the human great saphenous vein used for venoplasty of rat IVC [36]. Their decellularized grafts were conjugated with hyaluronic acid and heparin prior to the implantation and compared with only decellularized non-coated patches of the same origin. They demonstrated that these coated decellularized patches had significantly thinner neointima compared to the uncoated patches. The intimal hyperplasia was also documented in their previous studies with pericardium patches [61, 62]. There were no signs of intimal hyperplasia in our experiments. As one of the main factors responsible for intimal hyperplasia is increased or decreased shear stress on the vascular wall [63], we conclude that intimal hyperplasia could be prevented by orthotopic implantation of decellularised venous grafts. In such situation, the physiologic perfusion is maintained and intimal hyperplasia does not occur even without any additional coating of decellularised grafts.

4.6 Thrombosis

The rate of thrombosis in our study was 12.5% in the cryopreserved grafts and 33.3% in the decellularized grafts. There is a limited number of studies describing implantation of decellularized venous grafts without any further modification in venous system. Therefore, the comparison of our results is limited. Hakkanson et al. presented 100% patency after vena cava reconstruction with decellularized caval vein grafts previously perfused by the recipient blood [37]. However, the pre-treatment with the recipient's blood was not the only difference from our model. Anticoagulation (rivaroxaban) and anti-aggregation (acetylsalicylic acid) were used in their study during the whole postoperative period [37]. Yamanaka et al. examined decellularized venous grafts of small diameter that were modified with integrin $\alpha 4\beta 1$ ligand (with affinity for endothelial cells) and implanted in venous system. The authors did not mention the use of anticoagulation and they observed 62% patency after 6 months [64]. The limited graft patency in our study could be attributed to the omission of anticoagulation or anti-aggregation in the postoperative period. In our previous study focused on portal vein reconstruction with cold-stored venous allografts, we noted portal vein thrombosis in 19.2% when using the same breed of domestic pig and also no postoperative anticoagulation [57]. Decellularized veins implanted in arterial system usually show good patency. Decellularized jugular veins used as grafts implanted in the carotid artery in the canine model showed a 100% patency after 2 or 8 weeks [31, 32]. The endothelization was present only in the perianastomotic regions and the rest of the lumen was covered with a compact fibrin layer [32]. As stated in the aims, our goal was to investigate the spontaneous in vivo recellularization, not to primarily find alternative grafts for vein reconstruction. Therefore, we designed a model with minimal influence on the blood-contact interface of the grafts with intent not to alter any cell adhesion processes. Animals in our experiment received only one bolus of heparin during the operation, but no anticoagulation or anti-aggregation was used in the postoperative period.

4.7 Limitations of the study

The limitation of this study is the short-term survival period. The wall of decellularized graft was similar to the wall of the native vein 28 days after implantation. However, potential long-term changes of the graft cannot be excluded. Another limitation is the thrombosis in some of the grafts not allowing their proper quantitative histologic evaluation. At least these grafts were examined before implantation and did not differ from the non-occluded grafts. The relatively high rate of thrombosis in this study is presumably influenced by the omitting of any anticoagulation or anti-aggregation postoperatively. As described above, it was done on purpose not to influence the cell adhesion process and recellularization itself. Further studies would be needed to evaluate the effect of anticoagulation or anti-aggregation specifically.

5 Conclusion

This study proves sufficient functionality of decellularized IVC grafts enabling their in situ recellularization. 28 days after orthotopic implantation these grafts had a similar structure as the native IVC, and the immunogenicity of these grafts was substantially lower compared to the allogeneic cellular grafts. In situ recellularization has the potential to contribute to the development of artificial organs based on decellularized ECM without the need for full pre-transplant recellularization. It could also help to evaluate the quality of ECM and identify the cells attracted by the scaffold which is crucial for further tissue engineering research.

Acknowledgements Skillful technical support from Jana Dosoudilova and Jan Javurek is gratefully acknowledged for histological samples preparation.

Author contributions Conceptualization: R. Palek., V. Liska., L. Cervenkova, M.S. Massaro, V. Moulisova; methodology: R. Palek, M.S. Massaro, L. Cervenkova, M. Grajciarova., A. Maleckova; investigation—experimentation R. Palek, J. Rosendorf, R. Polak, S. Sarcevic, J. Sevcik, L. Kepkova, E. Korcakova, H. Mirka; data analysis: M. Grajciarova., A. Maleckova, E. Korcakova, H. Mirka, P. Hosek; writing—original draft preparation: R. Palek, M. Grajciarova, A. Maleckova; writing—review and editing: Z. Tonar, V. Liska. All authors have read and agreed to publish the manuscript.

Funding This work was supported by the project of Charles University in Prague (GAUK No. 462520), the project of the Ministry of Health of the Czech Republic (AZV NU22J-06-00058), and Charles University in Prague programs (START/MED/027 Start Program No. CZ.02.2.69/0.0/0.0/19_073/00169 35, program Cooperatio “Surgical Disciplines” no. 207043 and Cooperatio Program, research area MED/DIAG).

Data availability The data that support the findings of this study are available from the corresponding author upon reasonable request.

Code availability Not applicable.

Declarations

Ethics approval and consent to participate The protocol of in vivo experiment was approved and controlled by the Ministry of Education, Youth and Sports of the Czech Republic (project code: MSMT-18870/2020–3). All the procedures involving animals were performed in compliance with the law of the Czech Republic, which is compatible with the legislation of the European Union (EU Directive 2010/63/EU for animal experiments).

Competing interests The authors declare that there is no conflict of interest in connection with this article.

Open Access This article is licensed under a Creative Commons Attribution 4.0 International License, which permits use, sharing, adaptation, distribution and reproduction in any medium or format, as long as you give appropriate credit to the original author(s) and the source, provide a link to the Creative Commons licence, and indicate if changes were made. The images or other third party material in this article are included in the article's Creative Commons licence, unless indicated otherwise in a credit line to the material. If material is not included in the article's Creative Commons licence and your intended use is not permitted by statutory regulation or exceeds the permitted use, you will need to obtain permission directly from the copyright holder. To view a copy of this licence, visit <http://creativecommons.org/licenses/by/4.0/>.

References

1. Guruswamy Damodaran R, Vermette P. Tissue and organ decellularization in regenerative medicine. *Biotechnol Prog.* 2018;34(6):1494–505.

2. García-Gareta E, Abduldaiem Y, Sawadkar P, Kyriakidis C, Lali F, Greco KV. Decellularised scaffolds: Just a framework? Current knowledge and future directions. *J Tissue Eng.* 2020;11:2041731420942903.
3. Zhang X, Chen X, Hong H, Hu R, Liu J, Liu C. Decellularized extracellular matrix scaffolds: recent trends and emerging strategies in tissue engineering. *Bioact Mater.* 2022;10:15–31.
4. Petersen TH, Calle EA, Zhao L, Lee EJ, Gui L, Raredon MB, Gavrilov K, Yi T, Zhuang ZW, Breuer C, Herzog E, Niklason LE. Tissue-engineered lungs for in vivo implantation. *Science.* 2010;329(5991):538–41.
5. Ott HC, Matthiesen TS, Goh SK, Black LD, Kren SM, Netoff TI, Taylor DA. Perfusion-decellularized matrix: using nature's platform to engineer a bioartificial heart. *Nat Med.* 2008;14(2):213–21.
6. Song JJ, Guyette JP, Gilpin SE, Gonzalez G, Vacanti JP, Ott HC. Regeneration and experimental orthotopic transplantation of a bioengineered kidney. *Nat Med.* 2013;19(5):646–51.
7. Uygun BE, Soto-Gutierrez A, Yagi H, Izamis ML, Guzzardi MA, Shulman C, Milwid J, Kobayashi N, Tilles A, Berthiaume F, Hertl M, Nahmias Y, Yarmush ML, Uygun K. Organ reengineering through development of a transplantable recellularized liver graft using decellularized liver matrix. *Nat Med.* 2010;16(7):814–20.
8. Moulisová V, Jiřík M, Schindler C, Červenková L, Pálek R, Rosendorf J, Arlt J, Bolek L, Šušová S, Nietzsche S, Liška V, Dahmen U. Novel morphological multi-scale evaluation system for quality assessment of decellularized liver scaffolds. *J Tissue Eng.* 2020;11:2041731420921121.
9. Kheir E, Stapleton T, Shaw D, Jin Z, Fisher J, Ingham E. Development and characterization of an acellular porcine cartilage bone matrix for use in tissue engineering. *J Biomed Mater Res A.* 2011;99(2):283–94.
10. Teebken OE, Bader A, Steinhoff G, Haverich A. Tissue engineering of vascular grafts: human cell seeding of decellularised porcine matrix. *Eur J Vasc Endovasc Surg.* 2000;19(4):381–6.
11. Badylak SF, Tullius R, Kokini K, Shelbourne KD, Klootwyk T, Voytik SL, Kraine MR, Simmons C. The use of xenogeneic small intestinal submucosa as a biomaterial for Achilles tendon repair in a dog model. *J Biomed Mater Res.* 1995;29(8):977–85.
12. Shaheen MF, Joo DJ, Ross JJ, Anderson BD, Chen HS, Huebert RC, Li Y, Amiot B, Young A, Zlochiver V, Nelson E, Mounajjed T, Dietz AB, Michalak G, Steiner BG, Davidow DS, Paradise CR, van Wijnen AJ, Shah VH, Liu M, Nyberg SL. Sustained perfusion of revascularized bioengineered livers heterotopically transplanted into immunosuppressed pigs. *Nat Biomed Eng.* 2020;4(4):437–45.
13. Dias ML, Paranhos BA, Goldenberg R. Liver scaffolds obtained by decellularization: a transplant perspective in liver bioengineering. *J Tissue Eng.* 2022;13:20417314221105304.
14. Edgar L, Pu T, Porter B, Aziz JM, La Pointe C, Asthana A, Orlando G. Regenerative medicine, organ bioengineering and transplantation. *Br J Surg.* 2020;107(7):793–800.
15. Kim JJ, Hou L, Huang NF. Vascularization of three-dimensional engineered tissues for regenerative medicine applications. *Acta Biomater.* 2016;41:17–26.
16. Pashneh-Tala S, MacNeil S, Claeysens F. The tissue-engineered vascular graft-past present, and future. *Tissue Eng Part B Rev.* 2016;22(1):68–100.
17. Hasse B, Husmann L, Zinkernagel A, Weber R, Lachat M, Mayer D. Vascular graft infections. *Swiss Med Wkly.* 2013;143: w13754.
18. Weiss S, Bachofen B, Widmer MK, Makaloski V, Schmidli J, Wyss TR. Long-term results of cryopreserved allografts in aortoiliac graft infections. *J Vasc Surg.* 2021;74(1):268–75.
19. Madden RL, Lipkowitz GS, Browne BJ, Kurbanov A. Experience with cryopreserved cadaveric femoral vein allografts used for hemodialysis access. *Ann Vasc Surg.* 2004;18(4):453–8.
20. Lehr EJ, Rayat GR, Chiu B, Churchill T, McGann LE, Coe JY, Ross DB. Decellularization reduces immunogenicity of sheep pulmonary artery vascular patches. *J Thorac Cardiovasc Surg.* 2011;141(4):1056–62.
21. Della Schiava N, Mathevet JL, Boudjelit T, Arsicot M, Feugier P, Lermusiaux P, Millon A. Cryopreserved arterial allografts and abo and rhesus compatibility. *Ann Vasc Surg.* 2016;33:173–80.
22. Kim BS, Das S, Jang J, Cho DW. Decellularized extracellular matrix-based bioinks for engineering tissue- and organ-specific microenvironments. *Chem Rev.* 2020;120(19):10608–61.
23. Shi J, Teng Y, Li D, He J, Midgley AC, Guo X, Wang X, Yang X, Wang S, Feng Y, Lv Q, Hou S. Biomimetic tri-layered small-diameter vascular grafts with decellularized extracellular matrix promoting vascular regeneration and inhibiting thrombosis with the salidroside. *Mater Today Bio.* 2023;21: 100709.
24. Niklason LE. Understanding the extracellular matrix to enhance stem cell-based tissue regeneration. *Cell Stem Cell.* 2018;22(3):302–5.
25. Massaro MS, Pálek R, Rosendorf J, Červenková L, Liška V, Moulisová V. Decellularized xenogeneic scaffolds in transplantation and tissue engineering: Immunogenicity versus positive cell stimulation. *Mater Sci Eng C Mater Biol Appl.* 2021;127: 112203.
26. Sarikouch S, Theodoridis K, Hilfiker A, Boethig D, Laufer G, Andreas M, Cebotari S, Tudorache I, Bobylev D, Neubert L, Teiken K, Robertus JL, Jonigk D, Beerbaum P, Haverich A, Horke A. Early insight into in vivo recellularization of cell-free allogenic heart valves. *Ann Thorac Surg.* 2019;108(2):581–9.
27. Kurokawa S, Hashimoto Y, Funamoto S, Murata K, Yamashita A, Yamazaki K, Ikeda T, Minatoya K, Kishida A, Masumoto H. In vivo recellularization of xenogeneic vascular grafts decellularized with high hydrostatic pressure method in a porcine carotid arterial interpose model. *PLoS ONE.* 2021;16(7): e0254160.
28. Sakakibara S, Ishida Y, Hashikawa K, Yamaoka T, Terashi H. Intima/medulla reconstruction and vascular contraction-relaxation recovery for acellular small diameter vessels prepared by hyperosmotic electrolyte solution treatment. *J Artif Organs.* 2014;17(2):169–77.
29. Hwang SJ, Kim SW, Choo SJ, Lee BW, Im IR, Yun HJ, Lee SK, Song H, Cho WC, Lee JW. The decellularized vascular allograft as an experimental platform for developing a biocompatible small-diameter graft conduit in a rat surgical model. *Yonsei Med J.* 2011;52(2):227–33.
30. Assmann A, Delfs C, Munakata H, Schiffer F, Horstkötter K, Huynh K, Barth M, Stoldt VR, Kamiya H, Boeken U, Lichtenberg A, Akhyari P. Acceleration of autologous in vivo recellularization of decellularized aortic conduits by fibronectin surface coating. *Biomaterials.* 2013;34(25):6015–26.
31. Schaner PJ, Martin ND, Tulenko TN, Shapiro IM, Tarola NA, Leichter RF, Carabasi RA, Dimuzio PJ. Decellularized vein as a potential scaffold for vascular tissue engineering. *J Vasc Surg.* 2004;40(1):146–53.
32. Martin ND, Schaner PJ, Tulenko TN, Shapiro IM, Dimatteo CA, Williams TK, Hager ES, DiMuzio PJ. In vivo behavior of decellularized vein allograft. *J Surg Res.* 2005;129(1):17–23.

33. Assmann A, Akhyari P, Delfs C, Flögel U, Jacoby C, Kamiya H, Lichtenberg A. Development of a growing rat model for the in vivo assessment of engineered aortic conduits. *J Surg Res.* 2012;176(2):367–75.
34. Hilbert SL, Boerboom LE, Livesey SA, Ferrans VJ. Explant pathology study of decellularized carotid artery vascular grafts. *J Biomed Mater Res A.* 2004;69(2):197–204.
35. Lin CH, Hsia K, Ma H, Lee H, Lu JH. In vivo performance of decellularized vascular grafts: a review article. *Int J Mol Sci.* 2018;19(7):2101.
36. Bai H, Wang Z, Li M, Liu Y, Wang W, Sun P, Wei S, Wang Z, Li J, Dardik A. Hyaluronic acid-heparin conjugated decellularized human great saphenous vein patches decrease neointimal thickness. *J Biomed Mater Res B Appl Biomater.* 2020;108(6):2417–25.
37. Håkansson J, Simsa R, Bogestål Y, Jenndahl L, Gustafsson-Hedberg T, Petronis S, Strehl R, Österberg K. Individualized tissue-engineered veins as vascular grafts: a proof of concept study in pig. *J Tissue Eng Regen Med.* 2021;15(10):818–30.
38. Österberg K, Bogestål Y, Jenndahl L, Gustafsson-Hedberg T, Synnergren J, Holmgren G, Bom E, Petronis S, Krona A, Eriksson JS, Rosendahl J, Crisostomo V, Sanchez-Margallo FM, Baez-Diaz C, Strehl R, Håkansson J. Personalized tissue-engineered veins—long term safety, functionality and cellular transcriptome analysis in large animals. *Biomater Sci.* 2023;11(11):3860–77.
39. Kolinko Y, Malečková A, Kochová P, Grajciarová M, Blassová T, Kural T, Trailin A, Červenková L, Havránková J, Vištejnová L, Tonarová P, Moulisová V, Jiřík M, Zavadáková A, Tichánek F, Liška V, Králíčková M, Witter K, Tonar Z. Using virtual microscopy for the development of sampling strategies in quantitative histology and design-based stereology. *Anat Histol Embryol.* 2022;51(1):3–22.
40. Grajciarova M, Turek D, Maleckova A, Palek R, Liska V, Tomasek P, Kralickova M, Tonar Z. Are ovine and porcine carotid arteries equivalent animal models for experimental cardiac surgery: a quantitative histological comparison. *Ann Anat.* 2022;242: 151910.
41. Tomášek P, Tonar Z, Grajciarová M, Kural T, Turek D, Horáková J, Pálek R, Eberlová L, Králíčková M, Liška V. Histological mapping of porcine carotid arteries—an animal model for the assessment of artificial conduits suitable for coronary bypass grafting in humans. *Ann Anat.* 2020;228: 151434.
42. Tonar Z, Kochova P, Cimrman R, Perktold J, Witter K. Segmental differences in the orientation of smooth muscle cells in the tunica media of porcine aortae. *Biomech Model Mechanobiol.* 2015;14(2):315–32.
43. H V, M R. *Unbiased stereology: three-dimensional measurement in microscopy*, 2nd Edition ed., Garland Science, London;2004
44. Tschanz S, Schneider JP, Knudsen L. Design-based stereology: planning, volumetry and sampling are crucial steps for a successful study. *Ann Anat.* 2014;196(1):3–11.
45. Gundersen HJG. Notes on the estimation of the numerical density of arbitrary profiles: the edge effect. *J Microsc.* 1977;111(2):219–23.
46. Nafe R, Schlote W, Schneider B. Histo-morphometry of tumour cell nuclei in astrocytomas using shape analysis, densitometry and topometric analysis. *Neuropathol Appl Neurobiol.* 2005;31(1):34–44.
47. Drougas JG, Barnard SE, Wright JK, Sika M, Lopez RR, Stokes KA, Williams PE, Pinson CW. A model for the extended studies of hepatic hemodynamics and metabolism in swine. *Lab Anim Sci.* 1996;46(6):648–55.
48. Breuer S, Fogelstrand P, Lindskog H, Osterberg K, Luebke T, Brunkwall J, Mattsson E. Introduction of embryonic stem cells into vein grafts reduces intimal hyperplasia in mice. *J Cardiovasc Surg (Torino).* 2014;55(2):235–46.
49. Piola M, Soncini M, Prandi F, Polvani G, Beniamino Fiore G, Pesce M. Tools and procedures for ex vivo vein arterialization, preconditioning and tissue engineering: a step forward to translation to combat the consequences of vascular graft remodeling. *Recent Pat Cardiovasc Drug Discov.* 2012;7(3):186–95.
50. Olausson M, Patil PB, Kuna VK, Chougule P, Hernandez N, Methe K, Kullberg-Lindh C, Borg H, Ejnell H, Sumitran-Holgersson S. Transplantation of an allogeneic vein bioengineered with autologous stem cells: a proof-of-concept study. *Lancet.* 2012;380(9838):230–7.
51. Crapo PM, Gilbert TW, Badylak SF. An overview of tissue and whole organ decellularization processes. *Biomaterials.* 2011;32(12):3233–43.
52. Kahle B, Schmidtko C, Hunzelmann N, Bartels C, Sievers HH, Steenbock H, Reinhardt DP, Brinckmann J. The extracellular matrix signature in vein graft disease. *Can J Cardiol.* 2016;32(8):1008.e11–7.
53. Ozturk N, Sucu N, Comelekoglu U, Yilmaz BC, Aytacoglu BN, Vezir O. Pressure applied during surgery alters the biomechanical properties of human saphenous vein graft. *Heart Vessels.* 2013;28(2):237–45.
54. Yan S, Zhang Q, Cai M, Yu D, Chen J, Yu P, Zhao Q, Zhou L, Hoffmann M, Zheng S. A novel model of portal vein transplantation in mice using two-cuff technique. *Microsurgery.* 2007;27(6):569–74.
55. Glowinski S, Bańkowski E. Content and distribution of collagen in venous and polyester aortal grafts. *Atherosclerosis.* 1982;41(1):125–31.
56. Wong AP, Nili N, Jackson ZS, Qiang B, Leong-Poi H, Jaffe R, Raanani E, Connelly PW, Sparkes JD, Strauss BH. Expansive remodeling in venous bypass grafts: novel implications for vein graft disease. *Atherosclerosis.* 2008;196(2):580–9.
57. Palek R, Jonasova A, Rosendorf J, Mik P, Bajcurova K, Hosek P, Moulisova V, Eberlova L, Haidingerova L, Brzon O, Bednar L, Kriz T, Dolansky M, Treska V, Tonar Z, Vimmer J, Liska V. Allogeneic venous grafts of different origin used for portal vein reconstruction after pancreaticoduodenectomy—experimental study. *Anticancer Res.* 2019;39(12):6603–20.
58. Carpenter JP, Tomaszewski JE. Human saphenous vein allograft bypass grafts: immune response. *J Vasc Surg.* 1998;27(3):492–9.
59. Abrahimi P, Liu R, Pober JS. Blood vessels in allotransplantation. *Am J Transplant.* 2015;15(7):1748–54.
60. Graney PL, Ben-Shaul S, Landau S, Bajpai A, Singh B, Eager J, Cohen A, Levenberg S, Spiller KL. Macrophages of diverse phenotypes drive vascularization of engineered tissues. *Sci Adv.* 2020;6(18):eaay6391.
61. Bai H, Wang M, Foster TR, Hu H, He H, Hashimoto T, Hanisch JJ, Santana JM, Xing Y, Dardik A. Pericardial patch venoplasty heals via attraction of venous progenitor cells. *Physiol Rep.* 2016;4(12):e12841.
62. Bai H, Li X, Hashimoto T, Hu H, Foster TR, Hanisch JJ, Santana JM, Dardik A. Patch angioplasty in the rat aorta or inferior vena cava. *J Vis Exp.* 2017;120:e55253.
63. Wallitt EJ, Jevon M, Hornick PI. Therapeutics of vein graft intimal hyperplasia: 100 years on. *Ann Thorac Surg.* 2007;84(1):317–23.
64. Yamanaka H, Mahara A, Morimoto N, Yamaoka T. REDV-modified decellularized microvascular grafts for arterial and venous reconstruction. *J Biomed Mater Res A.* 2022;110(3):547–58.